Teoría de scattering de n fotones con m qubits en guías de onda

Advisors: Luis Martín Moreno & David Zueco Láinez

Universidad de Zaragoza - Máster en Física y Tecnologías Físicas
Université de Cergy-Pontoise - Master in Theoretical Physics and Applications

Curso 2012/2013

—

Eduardo Sánchez Burillo

June 24, 2013

Abstract

Light-matter interaction problem is for sure one of the most important topics in physics. Nowadays it is possible to deal experimentally with few photons, where quantum effects arise. From a theoretical point of view, immediately, numerical approximated methods are necessary. During this work, we study the Matrix Product States (MPS) technique and its application to 1D light-matter interaction problems.

Contents

1 Introduction

Light-matter interaction is a highly important topic in physics. At the quantum level, it is a very rich field, since these systems have a lot of potential (or even real) applications in, for example, quantum cryptography, quantum computing, etc. One of the main problems is to be able to manipulate few photons in the laboratory. Then, in spite of the fact that the field is very interesting, it did not attract too much attention from the theoretical physics community because the theory could not be compared to experimental results.

Nevertheless, a lot of effort was put during the last decades from the experimental point of view and these systems are nowadays accessible. For example, interaction of a photon with a single molecule [1] or a superconducting qubit [2, 3] can be implemented in a laboratory, observation of interesting effects like Electromagnetic Induced Transparency (EIT) for a single photon was observed [4], or a problem so exotic as light propagating through a complex network [5] has been studied; even systems mimicking this dynamics, like quantum plasmonics ones [6], have been implemented experimentally, and characteristic quantum properties, like entanglement, have been observed. Consequently the theoretical research has increased exponentially.

When studying this kind of problems, usually the analytical models are continuous, but as soon as one wants to study more complicated problems, where analytical tools are not valid, numerical methods are necessary and they require a discretisation of the system, e.g., the space is not continuous but it is just a discrete set of points. Then, the problem becomes a many-body physics one on a lattice. A generic N sites (that is, a lattice with N constituents) state is given by:

$$|\Psi\rangle = \sum_{i_1,\dots,i_N=1}^{d_1,\dots,d_N} c_{i_1,\dots,i_N} |i_1,\dots,i_N\rangle, \tag{1}$$

where $\{|i\rangle\}_{i=1}^{d_n}$ is an orthonormal basis for the Hilbert space $\mathcal{H}_n$ of the single site n, $d_n = \dim(\mathcal{H}_n)$ and $c_{i_1,\dots,i_N} \in \mathbb{C}$. The Hilbert space of the whole system is $\mathcal{H} = \bigotimes_{n=1}^{N} \mathcal{H}_n$ and its dimension is $\dim(\mathcal{H}) = \prod_{n=1}^{N} d_n$. So, note that we need a number of coefficients which increases exponentially with the number of particles. For simplicity, we can consider $d_n = 2\ \forall n$ and $N = 1000$. Then, $\dim(\mathcal{H}) = 2^{1000} > 10^{300}$. We cannot work with such a large number of coefficients, since it is impossible to store them and, if it were possible, the computations would take unapproachable times. So, it is not possible to handle numerically with the exact expressions, but it is necessary to use approximated methods.

In this work we have used the MPS technique to study several light-matter interaction problems in 1D. In the chapter II, we introduce and develop the MPS method. In the chapter III, we present the results. Finally, we present some conclusions and future projects.

2 MPS

One of the most celebrated approximated methods in the case of 1D systems with short range interactions is that of Matrix Product States (MPS). As we will see, in the beginning it is shown that any many-body state can be written exactly in such a way that a set of matrices define it. After that, the way in which one takes wisely the approximation will be explained. Lastly, we explain how to deal with this kind of states.

2.1 Theoretical fundamentals

First of all, the set of coefficients $c_{i_1,\ldots,i_N}$ can be stored in a matrix $C_{i_1,(i_2,\ldots,i_N)}$. On the other hand, every matrix $n \times m$ admits a singular value decomposition (SVD) [7], that is, a matrix A can be written as:

$$A = U\Sigma V^{\dagger}, \tag{2}$$

where U is an unitary $n \times n$ matrix, Σ is a diagonal $n \times m$ matrix with non negative entries called singular values σ_i, and V is unitary $m \times m$. This is applied over C:

$$C_{i_1,(i_2,\ldots,i_N)} = \sum_{n_2=1}^{D_2} U_{i_1,n_2}\sigma_{n_2}V^*_{(i_2,\ldots,i_N),n_2}, \tag{3}$$

with $D_2 := \min\{d_1, d_2d_3\ldots d_N\}$. Now, we define $(A_1^{i_1})_{1,n_2} := U_{i_1,n_2}$ and $c'_{n_2,i_2,\ldots,i_N} := \sigma_{n_2}V^*_{(i_2,\ldots,i_N),n_2}$. Then, the state can be written as:

$$|\Psi\rangle = \sum_{i_1,\ldots,i_N=1}^{d_1,\ldots,d_N}\sum_{n_2=1}^{D_2}(A_1^{i_1})_{1,n_2}c'_{n_2,i_2,\ldots,i_N}|i_1,\ldots,i_N\rangle \tag{4}$$

We set $C'_{(n_2,i_2),(i_3,\ldots,i_N)} := c'_{n_2,i_2,\ldots,i_N}$ and we take the SVD of C':

$$C'_{(n_2,i_2),(i_3,\ldots,i_N)} = \sum_{n_3=1}^{D_3} U'_{(n_2,i_2),n_3}\sigma'_{n_3}V'^*_{(i_3,\ldots,i_N),n_3}, \tag{5}$$

with $D_3 = \min\{D_2d_2, d_3d_4...d_N\}$. As before, we set $(A_2^{i_2})_{n_2,n_3} := U_{(n_2,i_2),n_3}$ and $c''_{n_3,i_3,\ldots,i_N} := \sigma'_{n_3}V'^*_{(i_3,\ldots,i_N),n_3}$. Then:

$$|\Psi\rangle = \sum_{i_1,\ldots,i_N=1}^{d_1,\ldots,d_N}\sum_{n_2,n_3=1}^{D_2,D_3}(A_1^{i_1})_{1,n_2}(A_2^{i_2})_{n_2,n_3}c''_{n_3,i_3,\ldots,i_N}|i_1,\ldots,i_N\rangle \tag{6}$$

Repeating the same procedure again and again:

$$|\Psi\rangle = \sum_{i_1,\ldots,i_N=1}^{d_1,\ldots,d_N}\sum_{n_2,\ldots,n_N=1}^{D_2,\ldots,D_N}(A_1^{i_1})_{1,n_2}\ldots(A_{N-1}^{i_{N-1}})_{n_{N-1},n_N}c^{(N-1)}_{n_N,i_N}|i_1,\ldots,i_N\rangle \tag{7}$$

Now, defining $(A_N^{i_N})_{n_N,1} := c^{(N-1)}_{n_N,i_N}$:

$$|\Psi\rangle = \sum_{i_1,\ldots,i_N=1}^{d_1,\ldots,d_N}\sum_{n_2,\ldots,n_N=1}^{D_2,\ldots,D_N}(A_1^{i_1})_{1,n_2}(A_2^{i_2})_{n_2,n_3}\ldots(A_{N-1}^{i_{N-1}})_{n_{N-1},n_N}(A_N^{i_N})_{n_N,1}|i_1,\ldots,i_N\rangle \tag{8}$$

Note that the sums over $n_2,\ldots,n_N$ are in fact products of the matrices $A_1^{i_1}$, $A_2^{i_2}$, etc. Then, we rewrite the state:

$$|\Psi\rangle = \sum_{i_1,\ldots,i_N=1}^{d_1,\ldots,d_N}A_1^{i_1}\ldots A_N^{i_N}|i_1,\ldots,i_N\rangle \tag{9}$$

We have shown that every $c_{i_1,\ldots,i_N}$ can be written as a product of matrices $D_1 \times D_2, \ldots, D_N \times D_{N+1}$, with $D_1 = D_{N+1}(= 1$ in this case). This is called a matrix product state. Because of the way in which we have derived the MPS, $D_1 = 1$, but, in general, D_1 can take other values (e.g., when working with periodic boundary conditions). So, considering D_1 not necessarily equal to 1:

$$|\Psi\rangle = \sum_{i_1,\ldots,i_N=1}^{d_1,\ldots,d_N} \sum_{n_1,n_2,\ldots,n_N=1}^{D_1,D_2,\ldots,D_N} (A_1^{i_1})_{n_1,n_2} \ldots (A_N^{i_N})_{n_N,n_1} |i_1,\ldots,i_N\rangle, \tag{10}$$

but it is exactly the same as before, that is, a product of matrices, except finally we take the trace over the resultant matrix. Then:

$$|\Psi\rangle = \sum_{i_1,\ldots,i_N=1}^{d_1,\ldots,d_N} \mathrm{Tr}(A_1^{i_1} \ldots A_L^{i_N}) |i_1,\ldots,i_N\rangle \tag{11}$$

This is the most general form of a MPS. If a given element of A_m is $(A_m^{i_m})_{n_m,n_{m+1}}$, i_m is called the physical index corresponding to m, since it is related to the local Hilbert space, and the remaining ones are the virtual indices.

At the moment, this description is exact for a general many-body state, so it is useless in principle. For simplicity, let $d_i = d$ and $D_i = D$, $\forall i$. Then, one has dD^2N numbers to encode d^N coefficients, so, D will be an exponentially large number if we want the description to be exact. As it can be supposed, the approximated method will consist in a truncation of the matrix sizes D_i. The question is why we can give a reliable description by doing so.

When looking at the expression (3), D_2 is the maximum of $\{d_1, d_2 d_3 \ldots d_N\}$ (in principle, $d_2 d_3 \ldots d_N$), but some of the singular values could vanish. If χ_2 is the quantity of non-vanishing σ_i, one could truncate the value of D_2 to χ_2 and the description would be still exact. By repeating the same argument again and again, finally one achieves a state of the following type:

$$|\Psi\rangle = \sum_{i_1,\ldots,i_N=1}^{d_1,\ldots,d_N} \sum_{n_1,n_2,\ldots,n_N=1}^{\chi_1,\chi_2,\ldots,\chi_N} (A_1^{i_1})_{n_1,n_2} \ldots (A_N^{i_N})_{n_N,n_1} |i_1,\ldots,i_N\rangle \tag{12}$$

Then, if one has states of this type, it is possible to reduce the values of D_i to χ_i and, hopefully, one will not need anymore an exponential quantity of coefficients. What is more, the singular values could show a huge decay such that it would be possible to truncate D_i in such a way that the error committed would remain under control. Anyway, at the moment we do not know if the singular values follow this kind of behaviour. In order to shed light on it, it is not very hard to check that χ_i is the rank [1] of the reduced density matrices [2] corresponding to the subsystems consisting of the sites $\{1,\ldots,i\}$ and

[1] Recall: the rank of a matrix is the number of non vanishing eigenvalues.

[2] A quantum system can be described by a statistical mixture of pure states, which mathematically is represented by a density matrix [8].

$\{i+1, \ldots, N\}$ [3] if we consider 1D systems [9]. This is related to one of the most surprising properties of quantum systems: entanglement. A system consisting of two subsystems A and B is said to be entangled if the state is not a tensor product, that is, if it cannot be written in the following way:

$$|\Psi\rangle = |\Phi_A\rangle|\xi_B\rangle \tag{13}$$

If a system is entangled, there is not a pure state corresponding to each of the subsystems, but they are described by mixed states, that is, non trivial reduced density matrices. For sure, entanglement is one of the most genuine quantum characteristics, since if one has a classical system consisting of several subsystems, there is a definite state describing each one, instead of having statistical combinations.

Obviously, if χ is the rank of the density matrices, it is an increasing measurement of the entanglement: if it is one, the state is not entangled since the reduced density matrix corresponds to a pure state, whereas if it increases, the subsystems are further of being pure states, so the system becomes more and more entangled. χ has other interesting properties in such a way that it becomes a good entanglement measurement [9]. Then, coming back to the many-body state written as a MPS (12), we define $\chi = \max_i\{\chi_i\}$ as the entanglement measurement. It is reasonable to think that the description of a given slightly entangled state will be faithful if one truncates the values of D_i. Actually, χ is directly related to the Von Neumann entropy, probably the main entanglement measurement for pure states [10]:

$$S := -\mathrm{Tr}(\rho \log \rho), \tag{14}$$

where ρ is the reduced density matrix corresponding to one of the subsystems (S does not depend on which subsystem one chooses) and the basis of the logarithm uses to be 2 or e. The relation between χ and S is very close: χ sets an upper bound for the Von Neumann entropy [9]. S turns out to be the capital parameter to justify the MPS method: in [11] they prove that if we want to approximate the ground state of a 1D system with short range interactions by using a MPS, the value of $D = \max_i\{D_i\}$ is always bounded by the Von Neumann entropy in the sense that the distance between the most optimal MPS and the true ground state is exponentially small if D increases polynomially with the number of particles. It makes perfectly sense; what we are saying is that it is possible to simulate the system via classical computation (because we do not need an exponential quantity of resources) instead of needing quantum computation and it happens when entanglement is small enough, that is, when the system is not so far of being classical in some sense.

Thus, that is why MPS method works, even for slightly excited states or time evolution. On one hand, it is widely accepted that physical states live on a tiny subspace of the whole Hilbert space. For instance, when considering time evolution of a given state over a time which scales polynomially with the number of particles, the evolved state samples an exponentially small volume in Hilbert space [12]. On the other hand, ground states of

[3] If one has a system and considers a partition, the reduced density matrices corresponding to the subsystems have the same rank.

local Hamiltonians are slightly entangled, in connection to what we said in the previous paragraph. What is more, they follow the area law [13]. This law arose in the context of black holes theory [14], but it turned out to be a highly general law for quantum field theories and condensed matter physics [13]. It says that if we consider the entanglement entropy S_l between two parts of the system in such a way that the linear size of the boundary between both parts is l, S_l is proportional to the area: $S_l \sim l^{\mathcal{D}-1}$, where $\mathcal{D}$ is the spatial dimension, instead of increasing with the volume of the partition, as it does for a general state [4]. It confirms the fact that the ground states entanglement is small and it is even much smaller than that of random states. Obviously, the ground state belongs to the little subset of physical states, so it may be expected that the other physical states have small entanglement in such a way that χ increases with some polynomial of the number of sites.

MPS is highly related to some older methods, like Numerical Renormalization Group (NRG) [15] and Density Matrix Renormalization Group (DMRG) [16], which were very successful (mainly DMRG) for describing ground states of 1D quantum many-body systems with short range interactions, even though those methods were not very justified in the beginning. Those studies showed that the singular values of ground or even slightly excited states decay exponentially; in other words, these states are slightly entangled, which again is in agreement with the previous analysis.

It is important to remark that this method is just valid for 1D systems. On one hand, this is related to the area law, since it means that entanglement is smaller when the spatial dimension decreases. On the other hand, note that the construction of a MPS is adapted to the geometry because of the fact that D_i measures the entanglement between the piece of the chain at the left of i (including i) and the rest, whereas it does not have this meaning if the system has more dimensions. Anyway, there are similar methods well suited to higher dimensional cases [11], like Projected Entangled Pair States (PEPS) method, but they do not give so good results.

In order to illustrate all this stuff, dN numbers are needed to represent a product state and it agrees with $D = 1$, which is the minimum possible value for D; i.e., if no entanglement (remember that a product state does not have entanglement), D takes the smallest possible value.

Finally, we have argued that MPS represent well enough low-energy states of some kind of systems. In the following, we will explain how to compute expected values, consider time evolution, find ground states, write some simple states in its MPS form, etc.

2.2 Expected values

When one considers different operations with MPS, it is much easier to consider diagrammatic representations. A general coefficient $c_{i_1,\ldots,i_N}$, so the whole state, can be

[4] Critical systems have logarithmic corrections to the area law. In any case, the entropy is still much smaller than that of random states.

represented as a network, as it can be looked at the figure (1). There, the boxes are the tensors, the legs pointing up correspond to the physical indices and the others are the virtual ones. The reader can look at other examples of such representations in [17] and [18]. Anyway, it is not so hard to develop the relations by considering the general formula of a MPS, but having the graphical representations is useful to develop a deeper intuition. The coefficients of the state in the chosen basis are:

$$c_{i_1,\dots,i_N} = \mathrm{Tr}(A_1^{i_1} \dots A_N^{i_N}) = (A_1^{i_1})_{k_1,k_2}(A_2^{i_2})_{k2,k3} \dots (A_N^{i_N})_{k_N,k_1}, \tag{15}$$

that is, we have N tensors with three indices and we contract the virtual ones. Note that here the repeated indices are summed; from now on, we will consider this convention. Looking again at the figure (1), one can realise that a contraction corresponds to a link between the virtual indices of neighbours sites.

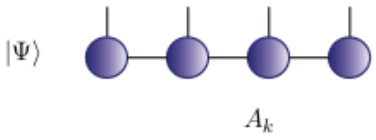

Figure 1: A general coefficient of a state with free boundary conditions is a set of boxes with three legs, except the first and the last ones, where the virtual legs are contracted. This image, and the others of this section, were taken from [18].

Now, if one computes, for example, the square of the norm, it is:

$$\langle\Psi|\Psi\rangle = c^*_{i_1,\dots,i_N} c_{i_1,\dots,i_N} = (A_1^{i_1})^*_{k_1,k_2}(A_2^{i_2})^*_{k2,k3} \dots (A_N^{i_N})^*_{k_N,k_1}(A_1^{i_1})_{l_1,l_2}(A_2^{i_2})_{l2,l3} \dots (A_N^{i_N})_{l_N,l_1} \tag{16}$$

So, it is just a contraction over the physical indices. The graphical representation is in the figure (2). Note that the physical indices are contracted. Then, we see that it is not necessary to compute all the coefficients, but it is possible to compute things like the norm by processing directly the tensors.

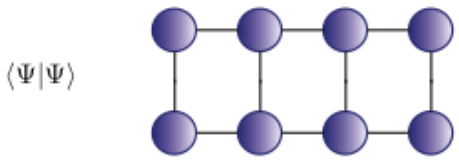

Figure 2: When considering the square of the norm, or, more generally, a scalar product, one has to take the graphical representation of both states and contract the physical indices.

On the other hand, usually an operator can be written as a sum of products of local operators, that is, a sum of objects like this:

$$O = O_1 \otimes O_2 \otimes \cdots \otimes O_N, \tag{17}$$

where O_n is an operator acting just on the site n. If $O_n^{i_n,j_n} := \langle i_n|O_n|j_n\rangle$ and $(E_n)_{i,j,k,l} := (A_n^{i_n})^*_{i,k} O_n^{i_n,j_n} (A_n^{j_n})_{j,l}$, where n is not summed, the expected value of such a product of local operators is:

$$\langle O\rangle = (A_1^{i_1})^*_{k_1,k_2} O_1^{i_1,j_1} (A_1^{j_1})_{l_1,l_2} (A_2^{i_2})^*_{k2,k3} O_2^{i_2,j_2} (A_2^{j_2})_{l2,l3} \ldots (A_N^{i_N})^*_{k_N,k_1} O_N^{i_N,j_N} (A_N^{j_N})_{l_N,l_1} \tag{18}$$

$$= (E_1)_{k_1,l_1,k_2,l_2} (E_2)_{k_2,l_2,k_3,l_3} \ldots (E_N)_{k_N,l_N,k_1,l_1} \tag{19}$$

Then, it is possible to compute the expected value of the typical operators without having to obtain explicitly the coefficients, just via the tensors. Now, the graphical representation is in (3). Note that each red box corresponds to one of the O_i and has two physical indices, which are contracted with the ones of $|\Psi\rangle$ and $\langle\Psi|$. Finally, this scheme can not be very efficient. In such a case, as we will explain later, an operator can be written in such a way (its MPO representation) that the expected value can be obtained directly, without having to decompose the operator in a sum of operators like (17).

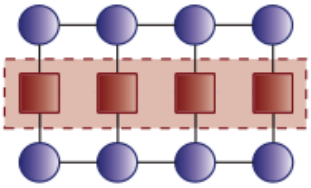

Figure 3: In this case, one contracts the physical indices of the state with those of the local operators.

2.3 Truncation procedure

One of the keys of the MPS technique is the truncation, that is, the approximation of a given state by a new one with smaller tensors. Theoretically, the problem is just to minimise the distance between the initial state $|\Psi\rangle$ (with tensors A_n) and a generic one with smaller tensors $|\Phi\rangle$ (with tensors B_n), that is, we want to minimise:

$$d^2(|\Psi\rangle, |\Phi\rangle) = (\langle\Psi| - \langle\Phi|)(|\Psi\rangle - |\Phi\rangle) = 1 + \langle\Phi|\Phi\rangle - 2\mathrm{Re}(\langle\Psi|\Phi\rangle) \tag{20}$$

Then, one has to compute $\langle\Phi|\Phi\rangle$ and $\langle\Psi|\Phi\rangle$ and both quantities are calculable. The question is how to minimise such a function in terms of the tensors of $|\Phi\rangle$. A possibility is to minimise it iteratively, that is, we start by the first site of the lattice. Then, all the tensors remain constant, except the one corresponding to the first site and the function is minimised with respect to B_1; after that, the tensors B_1, B_3, B_4, etc. remain constant and the function is minimised with respect to B_2, and so on. When minimising with respect to B_n, if v_n^Ψ and v_n^Φ are the vectorisations of A_n and B_n respectively, it can be shown (appendix A) that we have to minimise the following quadratic form:

$$f(A_n, B_n) = 1 + (v_n^\Phi)^\dagger E_1 v_n^\Phi - 2\mathrm{Re}\left((v_n^\Psi)^\dagger E_2 v_n^\Phi\right), \tag{21}$$

where E_1 and E_2 are matrices depending on the rest of tensors. Note that f is d^2, but its variables are just the tensors linked to the site n. f achieves its minimum value when v_n^Φ fulfils the following system of linear equations (the proof is omitted because it is trivial):

$$E_1 v_n^\Phi = E_2^\dagger v_n^\Psi \tag{22}$$

When the end of the chain is achieved, it is possible to come back in the opposite direction and realise a new sweep over the whole lattice, and so on, until some convergence criteria is fulfilled. For instance, when the distance takes a value smaller than a desired tolerance. As we indicated above, the reader can find how E_1 and E_2 are defined and more information about the truncation algorithm in the appendix A.

2.4 Time evolution

This part is based mainly on [19].

We are going to consider just the case where the Hamiltonian is time-independent. Then, the time evolution operator is:

$$U(t) = \exp(-iHt), \tag{23}$$

where we take $\hbar = 1$. In many-body physics, usually the Hamiltonians are:

$$H = \sum_{i=1}^{N} h_i, \tag{24}$$

where h_i takes into account the interaction between the site i and some of its neighbours. Here, we just consider the case where we have 2 bodies interaction between nearest neighbours, so h_i encodes the interaction between i and $i+1$ [5].

Computing $U(t)$ and applying it over a MPS is not feasible, because the result is not a MPS anymore. Then, we have to handle with some approximations. First of all, we split the Hamiltonian: $H = H_O + H_E$. The most typical option is to take H_O equal to the Hamiltonian corresponding to the odd links and H_E that corresponding to the even edges. Both of them are sums of commuting Hamiltonians, so, assuming N even:

$$\exp(-iH_O t) = \exp(-ih_1 t)\exp(-ih_3 t)\ldots\exp(-ih_{N-1} t) \tag{25}$$
$$\exp(-iH_E t) = \exp(-ih_2 t)\exp(-ih_4 t)\ldots\exp(-ih_N t) \tag{26}$$

Here, h_n takes into account the interaction between n and $n+1$, or it is a free Hamiltonian for the site n. Then, the application of $u_n(t) := \exp(-ih_n t)$ over a MPS is trivial [9]. In the case of one-body operators, once applied, the result is again a MPS. On the other hand, it is true that the new state is not a MPS if $u_n(t)$ is a two-body operator, since it mixes the tensors corresponding to the sites n and $n+1$, so the new state has a

[5] h_N considers the interaction between N and 1 if periodic boundary conditions (pbc) are implemented, whereas it is just a free Hamiltonian for the site N if free boundary conditions (fbc) are imposed.

tensor linked to the couple of sites $(n, n+1)$, whereas a MPS has a tensor corresponding to each site. However, a MPS is recovered by doing a singular value decomposition (SVD) of this new tensor.

Now, a question arises: how to express $\exp(-i(H_E + H_O)t)$ in terms of exponentials of H_E and H_O. With this purpose, we take hand of the Suzuki-Trotter decompositions. The second order one is:

$$\exp\left(-i(H_E + H_O)\Delta t\right) = \exp(-iH_E\Delta t)\exp(-iH_O\Delta t) + \mathcal{O}(\Delta t^2) \tag{27}$$

There are improved versions. For example, the third order one is:

$$\exp\left(-i(H_E + H_O)\Delta t\right) = \exp(-iH_E\Delta t/2)\exp(-iH_O\Delta t)\exp(-iH_E\Delta t/2) + \mathcal{O}(\Delta t^3) \tag{28}$$

In [19], there are versions until $\mathcal{O}(\Delta t^5)$. Now, the point is that, after applying the time evolution, the tensors are bigger than the ones of the initial state. Then, if we want to be able to handle with the evolved states, we have to truncate them, so we take hand of the truncation procedure explained above.

There exist other ways to implement the time evolution, as Runge Kutta and Arnoldi-like methods, for example. They are considered in [19].

2.4.1 Imaginary evolution

If one considers evolution with imaginary times (with negative imaginary part), the state tends to the ground state by normalising the final state. It is not difficult to see it. First, given a state, it can be decomposed as a sum of eigenstates of the Hamiltonian $\{|\phi_n\rangle\}$, whose eigenvalues $\{E_n\}$ are in increasing order starting at $n = 0$ (that is, the ground state is $|\phi_0\rangle$ and $E_0 < E_1 < \dots$):

$$|\Psi(0)\rangle = \sum_n c_n|\phi_n\rangle \tag{29}$$

If time evolution is applied:

$$|\Psi(t)\rangle = e^{-iHt}|\Psi(0)\rangle = \sum_n c_n e^{-iE_n t}|\phi_n\rangle \tag{30}$$

Now, if $t = -i\tau$, with $\tau \in \mathbb{R}^+$:

$$|\Psi(\tau)\rangle = \sum_n c_n e^{-E_n\tau}|\phi_n\rangle \tag{31}$$

Since the time evolution is not unitary in this case, we normalise again the state and we call it $|\varphi(\tau)\rangle$:

$$|\varphi(\tau)\rangle = \frac{|\Psi(\tau)\rangle}{\sqrt{\langle\Psi(\tau)|\Psi(\tau)\rangle}} = \frac{\sum_n c_n e^{-E_n\tau}|\phi_n\rangle}{\sqrt{\sum_m |c_m|^2 e^{-2E_m\tau}}} \tag{32}$$

Taking the limit $\tau \to \infty$, the leading terms both in the numerator and in the denominator are those corresponding to the ground state, that is, to $n, m = 0$. Then:

$$\lim_{\tau\to\infty}|\varphi(\tau)\rangle = \frac{c_0}{|c_0|}|\phi_0\rangle, \tag{33}$$

which is equal to the ground state. So, this is a useful tool to find ground states.

Knowing the ground state is really important for a lot of interesting problems. In our case, it will be necessary since experimental implementations of scattering problems work at extremely low temperatures, so, before sending the excitations, the wave guide is really close to the ground state.

As a final remark, there are other methods to find the ground state. For example, it is possible to minimise the expected value of the Hamiltonian [11].

2.5 Matrix Product Operators (MPO)

In the same way that a state can be written like a product of matrices, we can do the same for every operator O [20]:

$$O = \mathrm{Tr}(C_1^{i_1,j_1}C_2^{i_2,j_2}\dots C_L^{i_L,j_L})|i_1 i_2\dots i_L\rangle\langle j_1 j_2\dots j_L| \tag{34}$$

This is very useful, because it is possible to apply an operator over a MPS trivially and the result is still a MPS. Let's show it, by applying O over a general MPS $|\Psi\rangle$ (10):

$$\begin{aligned}
&O|\Psi\rangle = \\
&(C_1^{i_1,j_1})_{n_1,n_2}(A_1^{k_1})_{m_1,m_2}\dots(C_L^{i_L,j_L})_{n_L,n_1}(A_L^{k_L})_{m_L,m_1}|i_1\dots i_L\rangle\langle j_1\dots j_L|k_1\dots k_L\rangle = \\
&(C_1^{i_1,j_1})_{n_1,n_2}(A_1^{j_1})_{m_1,m_2}\dots(C_L^{i_L,j_L})_{n_L,n_1}(A_L^{j_L})_{m_L,m_1}|i_1\dots i_L\rangle
\end{aligned}$$

Defining now $(B_a^{i_a})_{[n_a,m_a],[n_{a+1},m_{a+1}]} := (C_a^{i_a,j_a})_{n_a,n_{a+1}}(A_a^{j_a})_{m_a,m_{a+1}}$, where $[n_a,m_a]$ and $[n_a,m_a]$ are dealt as single indices. Then:

$$O|\Psi\rangle = (B_1^{i_1})_{[n_1,m_1],[n_2,m_2]}(B_2^{i_2})_{[n_2,m_2],[n_3,m_3]}\dots(B_L^{i_L})_{[n_L,m_L],[n_1,m_1]}|i_1 i_2\dots i_L\rangle, \tag{35}$$

which is a MPS. Now, the question is if it is possible to write easily typical operators as MPO. In the case of sums of one-body or two-body operators, it is feasible with small size of the matrices. In the first case, the operator is:

$$O_1 = \sum_{n=1}^{L} X_n, \tag{36}$$

If $(X_n)_{i_n,j_n} := \langle i_n|X_n|j_n\rangle$, it can be shown trivially that the following matrices are valid:

$$C_n^{i_n,j_n} = \begin{pmatrix} \delta_{i_n,j_n} & 0 \\ (X_n)_{i_n,j_n} & \delta_{i_n,j_n} \end{pmatrix} \qquad n = 2,3,\dots,L-1, \tag{37}$$

whereas $C_1^{i_1,j_1} = ((X_1)_{i_1,j_1}, \delta_{i_1,j_1})$ and $C_L^{i_L,j_L} = (\delta_{i_L,j_L}, (X_L)_{i_L,j_L})^T$. In the case of two-body operators:

$$O_2 = \sum_{n=1}^{L} X_n Y_{n+1}, \tag{38}$$

it accepts this MPO representation:

$$C_n^{i_n,j_n} = \begin{pmatrix} \delta_{i_n,j_n} & 0 & 0 \\ (Y_n)_{i_n,j_n} & 0 & 0 \\ 0 & (X_n)_{i_n,j_n} & \delta_{i_n,j_n} \end{pmatrix} \qquad n = 2, 3, \ldots, L-1, \tag{39}$$

$C_1^{i_1,j_1} = (0, (X_1)_{i_1,j_1}, \delta_{i_1,j_1})$ and $C_L^{i_L,j_L} = (\delta_{i_L,j_L}, (Y_L)_{i_L,j_L}, 0)^T$. As before, $(Y_n)_{i_n,j_n}$ are the matrix elements of Y_n.

This is really useful for several reasons. First, when doing dynamics, we need to write the initial condition in its MPS representations and this can help us, as we will explain in the next subsection. On the other hand, as we said above, calculating expected values of some operators, like H^2, is not very efficient by using the standard procedure explained before. However, one can construct $|\Psi_H\rangle = H|\Psi\rangle$ if the system has just one and two-body terms. Then the square of the norm will be $\langle\Psi_H|\Psi_H\rangle = \langle H^2\rangle$.

2.6 Writing states as MPS

Given a state, if one wants to know its MPS representation, the general procedure is quite complicated (or impossible), because it is necessary to apply SVD over exponentially huge matrices. As we want to perform time evolution, we need to write the initial state as MPS. Luckily, there are some tools to write some kinds of states as MPS. In this section we consider some examples.

2.6.1 Product states

We start by the most simple case, that is, product states:

$$|\Psi\rangle = \sum_{i_1,i_2,\ldots,i_L=1}^{d_1,d_2,\ldots,d_L} c_{1,i_1} c_{2,i_2} \ldots c_{L,i_L} |i_1, i_2, \ldots, i_L\rangle \tag{40}$$

By comparing with (10), it is trivial that this state already is a matrix product state where $D = 1$ for all the matrices, with $A_i^{n_i} = c_{i,n_i}$.

2.6.2 Case with several excitations

When working with transport problems, the initial conditions do not use to be states so simple as the one used above. Usually, one considers a wave guide in its ground state and some incident bosons. In order to create an excitation, it is necessary to apply:

$$C = \sum_{n=1}^{L} c_n a_n^\dagger, \tag{41}$$

over the ground state of the chain. But C is a sum of one-body operators, so an excitation can be created by acting with this operator in its MPO representation over the desired state and the result will be still a MPS, as we explained in the last section. In the same way, if one wants to work with more excitations, one just has to apply more operators like C.

3 Physical systems

Once we have explained the method, we apply it to several physical problems about propagation of bosons through one-dimensional systems moving freely or coupled to qubits. The codes are written in MATLAB 7.9.0 (R2009b).

3.1 Tight Binding Model

First of all, we have studied the bosonic tight binding model. The Hamiltonian with fbc reads:

$$H = \epsilon \sum_{n=1}^{L} a_n^\dagger a_n - J \sum_{n=1}^{L-1} (a_n^\dagger a_{n+1} + a_{n+1}^\dagger a_n), \tag{42}$$

where ϵ is called the eigenenergy, J is the hopping constant and $\{a_n^\dagger\}$ ($\{a_n\}$) is the set of bosonic creation (annihilation) operators. It will be the cornerstone of our work, since it is the discretisation of the electromagnetic Hamiltonian in one dimension [6].

Here, the chosen basis is:

$$|i_1, i_2, \ldots, i_L\rangle = \frac{1}{\sqrt{i_1! i_2! \ldots i_L!}} (a_1^\dagger)^{i_1} (a_2^\dagger)^{i_2} \ldots (a_L^\dagger)^{i_L} |0\rangle \tag{43}$$

We consider an initial state belonging to the one excitation subspace. Concretely, we take the following one:

$$|\Psi(0)\rangle = a_1^\dagger |0\rangle \tag{44}$$

The time evolution of the system for a chain of length $L = 20$ was studied and it was compared to results obtained via exact diagonalisation of the Hamiltonian with Mathematica software. The agreement is really good (not shown).

Secondly, we study the case with two bosons in the same state in a chain of length $L = 60$. Concretely, we generate a state with 2 bosons with Gaussian profiles around a given momentum:

[6] Strictly, this is not true, since if k is the dimensionless momentum, the dispersion relation of the electromagnetic field says that ω_k is a linear function of k, whereas now it is $\omega_k = \epsilon - 2J \cos k$ if pbc are imposed. However, working around $k = \pi/2$, ω_k tends to be linear, so the description will fulfil that of the continuum model.

$$|\Psi\rangle = \frac{1}{\sqrt{2}} \sum_{n,m=1}^{L} c_n c_m a_n^\dagger a_m^\dagger |0\rangle, \tag{45}$$

with:

$$c_n = N \exp\left(-\frac{(n-n_0)^2}{2\sigma^2} + ik_0 n \right), \tag{46}$$

where N is a normalisation constant. We choose $k_0 = \pi/2$, $\sigma = 8$ and $n_0 = 12$. We plot $N_n = \langle a_n^\dagger a_n \rangle$ as a function of n for different values of time in (4). In this case, both bosons propagate freely. As the state is close to an eigenstate [7], the shape of the profile remains more or less constant. However, when it arrives to the boundary, it suffers interference effects, bounces and it recovers in broad strokes the original shape. Anyway, what happens after the reflection is not too important because we will not consider this kind of effects. In addition, we show the total number of excitations, that is, the sum of N_n for all n in (5). As it can be seen, it is always equal to 2.

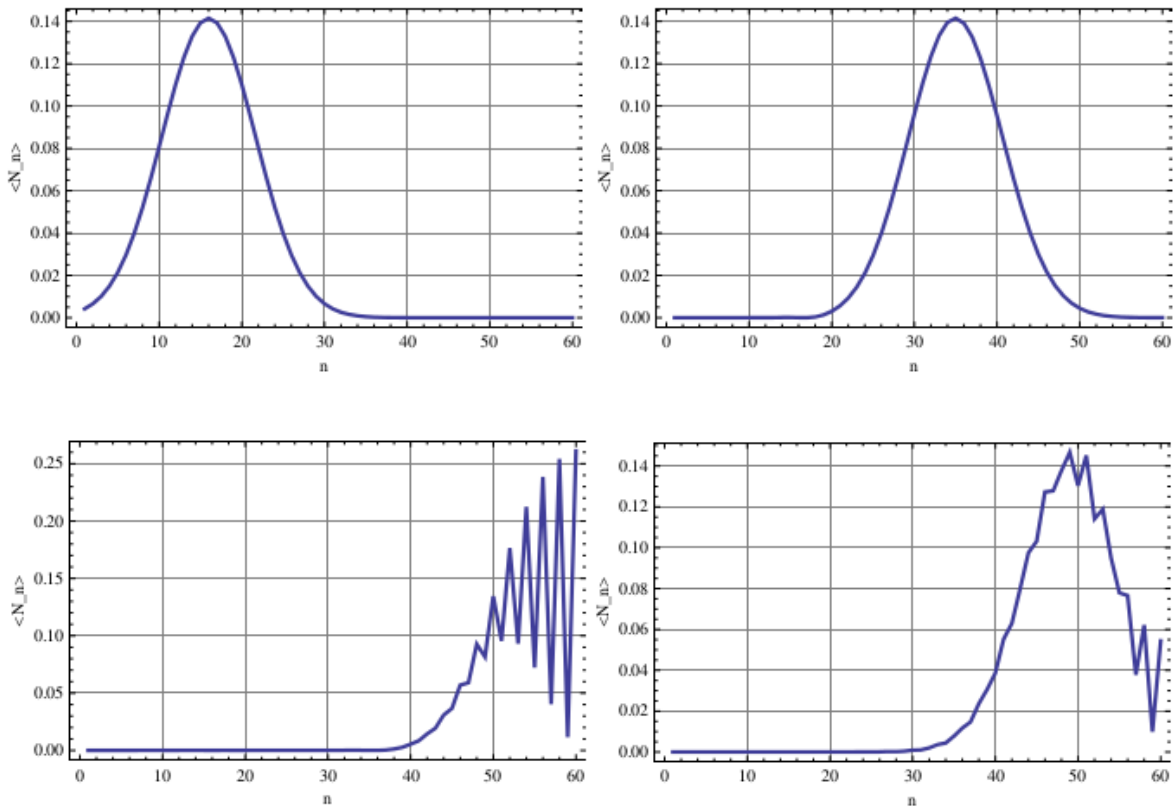

Figure 4: Number of excitations at $t = 0$, $t = 30$, $t = 60$ and $t = 90$ from left to right and from up to down.

[7] Remember that, if we had periodic boundary conditions and $\sigma \to \infty$, it would be an eigenstate, since it would be a state with definite momentum. In addition, if one looks at the discrete Fourier transform of c_n, the momentum distribution remains almost constant around $2k_0$ (not shown).

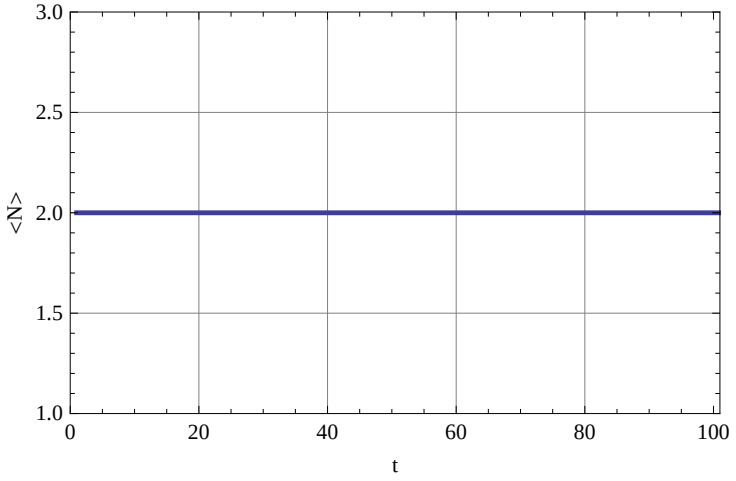

Figure 5: Total number of excitations

3.2 Decay of an excited qubit coupled to a tight binding model of bosons

After that, we applied the MPS method to a qubit coupled to a tight binding chain of bosons with dipole interaction. So, the Hamiltonian is:

$$H = \epsilon \sum_{n=1}^{L} a_n^\dagger a_n - J \sum_{n=1}^{L-1} (a_n^\dagger a_{n+1} + a_{n+1}^\dagger a_n) + \Omega \sigma^+ \sigma^- + g \sigma_x (a_{L_0}^\dagger + a_{L_0}), \tag{47}$$

where $L_0 = (L+1)/2$ (L is taken odd), Ω is the energy splitting of the qubit, g is the coupling constant between the qubit and the guide, σ_x is the Pauli matrix x and $\sigma^\pm$ are the ladder operators of the qubit. The interacting term is a point-like dipole interaction: first, the term $a_{L_0} + a_{L_0}^\dagger$ is the electric field in the Coulomb gauge [21]. On the other hand, we suppose that the square modulus of the wave functions corresponding to the states of the qubit $\psi_0(\mathbf{r}) := \langle \mathbf{r}|0\rangle$ and $\psi_1(\mathbf{r}) := \langle \mathbf{r}|1\rangle$ are even functions of $\mathbf{r}$, as well as the wave functions can be chosen as real ones. Taking into account that the dipole operator is proportional to $\mathbf{r}$, obviously its diagonal elements will vanish, whereas those non-diagonal will be equal. So, the matrix corresponding to the dipole operator is proportional to σ_x.

The used basis is the same as before (43), except for the site coupled to the qubit, where besides the usual states, we have to add those where the qubit is excited, that is, the local basis is $(a_{L_0}^\dagger)^{i_{L_0}} (\sigma^+)^n |0\rangle / \sqrt{i_{L0}!}$, with $n = 0$ or 1.

We consider the initial condition $|\Psi(0)\rangle = \sigma^+|0\rangle$, that is, there are not bosons and the qubit is excited. Even though $\langle \Psi(0)|N|\Psi(0)\rangle = 1$, this dynamics does not preserve the number of excitations, so in principle, it is necessary to consider the whole Hilbert space for the bosons. It would be an unapproachable problem, since the dimension of the space is infinite. However, for the parameters chosen here, it is more than enough with $d = 6$ (with except $d = 12$ for L_0, since the local Hilbert space is the one corresponding to the boson and the qubit).

Now, the local Hamiltonians are:

$$h_n = \epsilon a_n^\dagger a_n - J(a_n^\dagger a_{n+1} + a_n a_{n+1}^\dagger) \qquad (n \neq L, L_0) \tag{48}$$

$$h_{L_0} = \epsilon a_{L_0}^\dagger a_{L_0} - J(a_{L_0}^\dagger a_{L_0+1} + a_{L_0} a_{L_0+1}^\dagger) + \Omega\sigma^+\sigma^- + g\sigma_x(a_{L_0}^\dagger + a_{L_0}) \tag{49}$$

$$h_L = \epsilon a_L^\dagger a_L \tag{50}$$

We fix the size of the system to $L = 21$ (so $L_0 = 11$). We take $\epsilon = 1$, so the hopping factor is fixed to $J = 1/\pi$, since the dispersion relation becomes $\omega_k = 2k/\pi$. For the qubit we take $\Omega = 1$ and for the interaction $g = 0.05$ and $g = 0.5$. Other details of the simulations are: $\Delta t = 0.01$ and we consider the evolution until $t = 10$ and the tolerance is 10^{-6}, but the matrices are now allowed to increase, since it is necessary in the case of large g for the chosen tolerance.

The case with $g = 0.05$ is shown in the figure 6. The gray curve corresponds to the number of excitations and it remains almost equal to 1 (the corrections are at most around 10^{-4}). In such a case, when g/Ω is small enough, the rotating wave approximation (RWA) [22] works well enough; it consists in replacing $\sigma_x(a + a^\dagger)$ by $\sigma^+ a + \sigma^- a^\dagger$ (it is said that we are neglecting the counter rotating terms, $\sigma^- a + \sigma^+ a^\dagger$; in some sense, in this regime, these induce short time dynamics compared to the rotating terms). The number of excitations is a conserved quantity in this regime, which is in agreement with our results. On the other hand, the black curve corresponds to the population of the excited state of the qubit calculated with MPS. They have been compared to data obtained via exact diagonalisation by using Mathematica and the overlap between both data is total, as it is expected, since the RWA works really well in this case.

The case with $g = 0.50$ is plotted in 7. Again, the gray curve is the number of excitations and it does not remain constant, but it increases. So it is clear that the RWA does not work anymore when g/Ω is large enough. The black one is the population of the qubit computed with MPS. The agreement with [23] seems to be clear and the difference with the RWA results are obvious (not shown). In addition, as well as some of the excitations propagate, others stay close to the qubit, whereas in the case of low g/Ω, all the excitations propagate, nothing remains joined to the qubit (not shown).

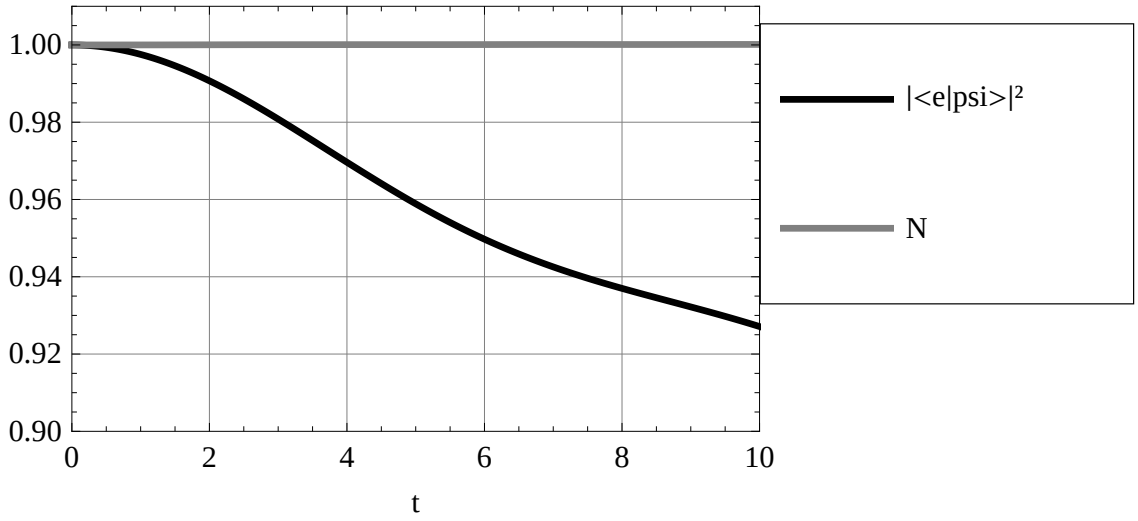

Figure 6: Number of excitations (gray) and qubit population (black) for $g = 0.05$

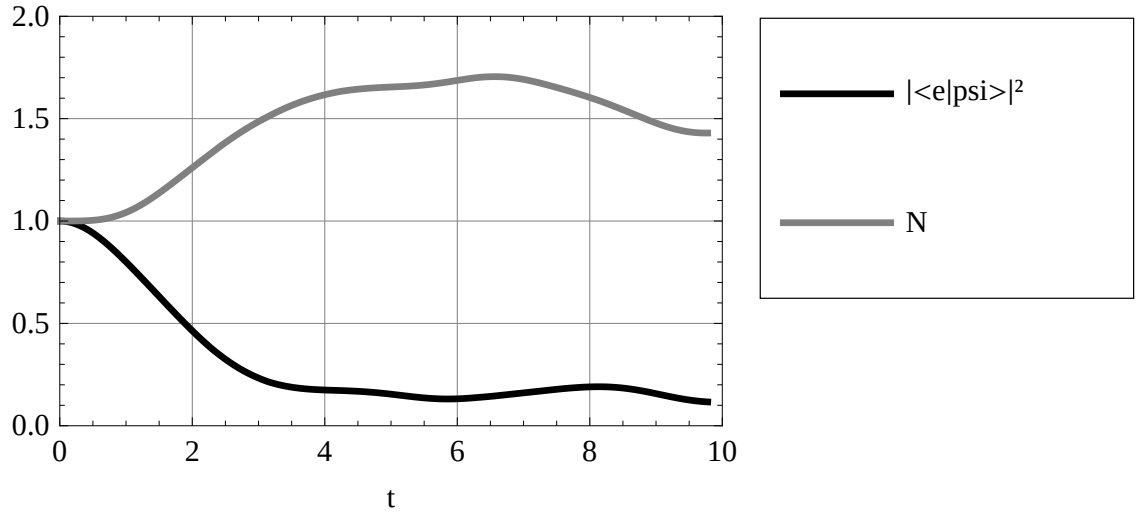

Figure 7: Number of excitations (gray) and qubit population (black) for $g = 0.50$

3.3 Scattering of an incident photon in the RWA regime

Now, we study the scattering problem in the RWA regime through different systems. First, we consider that the scatterer is a qubit and after that we shall deal with the case where there are 2 qubits in order to look for EIT.

3.3.1 One qubit

The Hamiltonian for a single qubit coupled to the chain is:

$$H = \epsilon \sum_{n=1}^{L} a_n^\dagger a_n - J \sum_{n=1}^{L-1} (a_n^\dagger a_{n+1} + a_n a_{n+1}^\dagger) + \Omega \sigma^+ \sigma^- + g(\sigma^- a_{L_0}^\dagger + \sigma^+ a_{L_0}) \qquad (51)$$

As it was said, the smaller is g/Ω, the better is the RWA. In addition, when considering this kind of problems, the closer is the energy of the incident wave packet to the qubit splitting (Ω), the finer is the approximation.

We choose $\epsilon = \Omega = 1$, $J = 1/\pi$, $g = 0.50$ [8], $L = 170$ and $L_0 = 90$. Here, the error remains under 10^{-12}, because the system stays in the one particle subspace. We take $\Delta t = 0.01$ and the final time is 230. As initial state we considered the qubit in its ground state and an incident Gaussian wave packet:

$$|\Psi(0)\rangle = \sum_n c_n a_n^\dagger |0\rangle, \qquad c_n = N \exp\left(-\frac{(n-n_0)^2}{2\sigma^2} + ik_0 n\right), \tag{52}$$

where $n_0 = 30$, $\sigma = 8$ and k_0 ranges along the set of values $\{\pi/2 - 0.5, \pi/2 - 0.4, \ldots, \pi/2 + 0.5\}$, since the interesting physical phenomena appear around the resonance and it happens when the energy corresponding to the wave packet is close to Ω. As $\omega_k = 1 - 2/\pi \cos k$ the resonance arises at $k_0 = \pi/2$.

What we measure is the qubit population as a function of time and the total current flowing between pairs of sites after and before the qubit position. This is just the time integral of the local current [24]

$$j_n(t) \propto i\langle (a_{n+1}^\dagger a_n - a_n^\dagger a_{n+1})\rangle \tag{53}$$

We do not care about the proportionality constant because we are interested in the transmission coefficient, which, for a general incident state $|\Psi\rangle$, is defined as the total transmitted current over the incident one, that is:

$$T(\Psi) := \frac{\int dt j_{n_2}(t)}{\int dt j_{n_1}(t)}, \tag{54}$$

where n_2 is a point beyond the qubit and n_1 is before the qubit. In the above definition, the integral domain is the time before the photon reflects. On the other hand, it can be computed analytically through the following expression:

$$T(\Psi) = \frac{\sum_k kT(k)|\Psi(k)|^2}{\sum_k k|\Psi(k)|^2}, \tag{55}$$

where k runs over $\pi(-1 + 2/L), \pi(-1 + 4/L), \ldots \pi$, $T(k)$ is the transmission coefficient for a monochromatic wave packet [25] and $\Psi(k) := \langle k|\Psi\rangle$.

The coefficient is shown in the figure (8) and it is compared to the analytical results. As it is seen, both data fit really well, but there are little errors (at most, the relative error achieves 5%) which are due to the time evolution algorithm. The interesting aspect is that the qubit tends to be transparent if the incident energy is far away of Ω, but it reflects almost totally the photon if it is resonant.

[8] It is true that there are not systems following the Hamiltonian (51); it is just an approximation working at small g/Ω. $g = 0.50\Omega$ is clearly out of the RWA regime. However, the intention of this part is to check our method with previous results and the computation time is smaller as g increases.

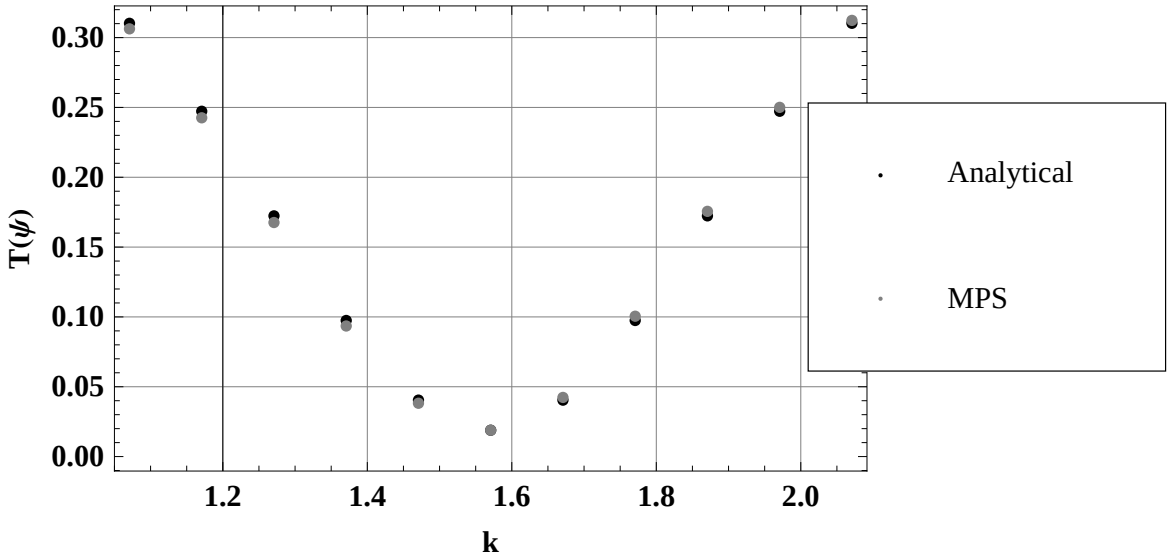

Figure 8: Transmission factor vs the central momentum for fixed $\sigma = 8$. The gray points correspond to those computed by means of MPS technique and the black ones are the analytical results.

The qubit population is shown for central momentum $\pi/2 - 0.5, \ldots, \pi/2$ in the figure (9) (for larger values it is not shown because for $\pi/2 + 0.1$ the result almost fits with that for $\pi/2 - 0.1$ and so on). As expected, the qubit excites and after that it relaxes to its ground state. The decay time is bigger if the wave packet is closer to the resonant case, as well as the maximum of the population increases in such a case.

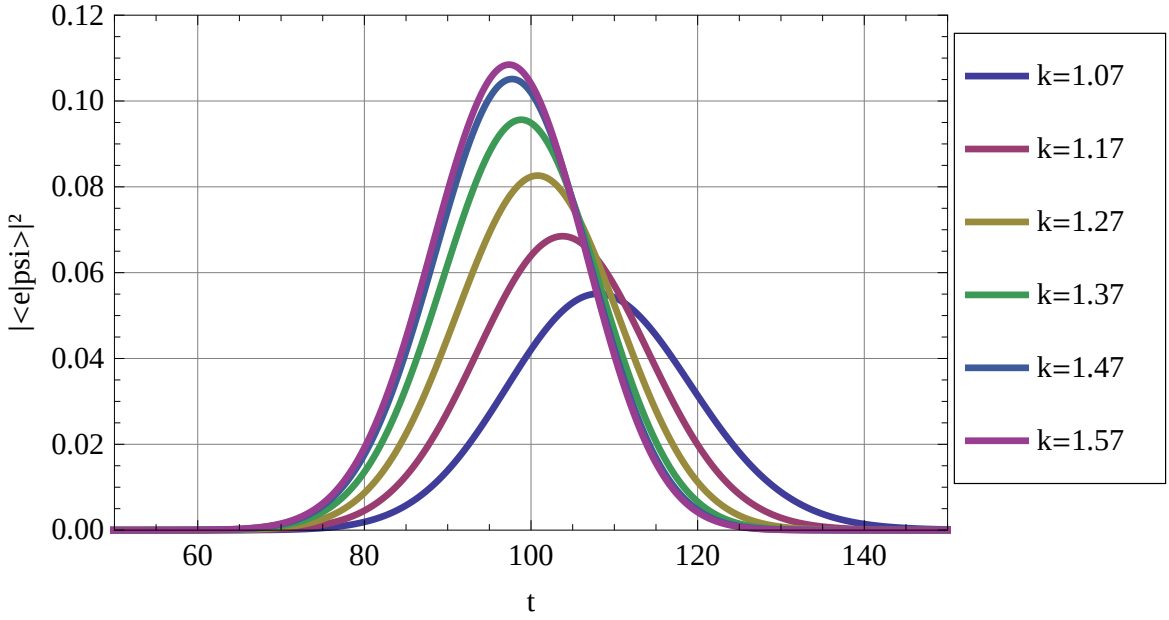

Figure 9: Qubit excited state population for several values of the central momentum. As it can be seen, the peak becomes narrower and higher as the wave packet energy is more resonant.

3.3.2 Electromagnetic Induced Transparency

Now, we consider a photon scattered by 2 different qubits separated by a distance d. In this case, again, if the incident energy is resonant with one of the qubits, then the photon reflects almost totally. However, a new effect appears: if the energy of the photon is in between the energies of both qubits, the pair of qubits becomes transparent.

The Hamiltonian is of course the same as before, but now there are 2 qubits instead of 1. The tight binding parameters are the same and those for the qubits are $\Omega_1 = 0.6$, $\Omega_2 = 1.4$ and $g_1 = g_2 = 0.5$. The length of the chain is $L = 220$ and the qubits positions are $L_1 = 109$ and $L_2 = 111$. The transmission coefficient is shown in the figure (10). The extremal values of the momentum correspond to the resonant cases with both qubits. In the middle, as we knew, a peak close to one appears (it becomes one for the monochromatic case). Again, the results are really close the analytical ones, computed with the transmission factor for this system [25].

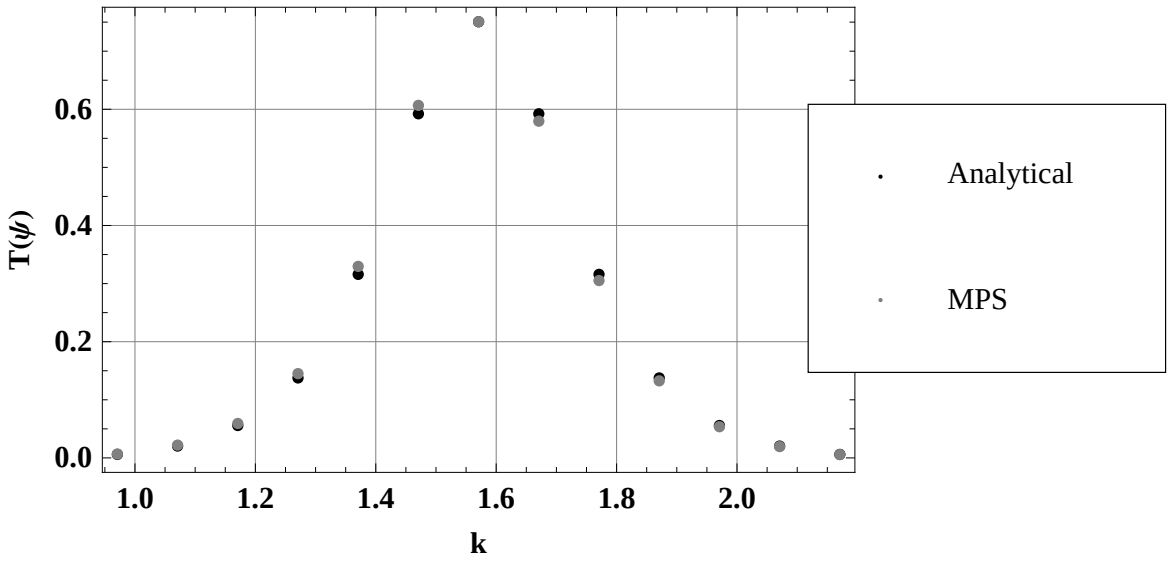

Figure 10: Transmission factor vs the central momentum for fixed $\sigma = 8$. The gray points correspond to those computed by means of MPS technique and the black ones are the analytical results.

3.4 Scattering in the ultra-strong regime

Here, we do not neglect the counter-rotating terms, that is, we work beyond the RWA so we take the Hamiltonian (47). First, we search the ground state and after that we study the scattering of a single excitation.

3.4.1 Ground state

As it was indicated, when studying scattering experiments, one works at really low temperatures, so the state of the wave guide before putting the excitations is really close to the ground one. Then we have to find it. Note that this is an interesting problem per

se; in fact, we have not found any previous work looking for it. We search it by using imaginary time evolution.

If g is small enough, the RWA works. In such a case, the ground state is that with no excitations: $|0\rangle$. However, it is clear that $|0\rangle$ is not an eigenstate of H if we do not neglect the counter rotating terms. In such a case, the RWA does not work anymore and the system belongs to the ultra-strong coupling regime. Immediately a question arises: are there physical systems working in this regime? The answer is yes. It is known that ordinary systems do not present a so huge coupling, but a lot of effort has been put during the last years and some sophisticated devices, like superconducting qubits, have shown ultra-strong regime [26], besides there are theoretical purposes to achieve even larger coupling constants [27].

For the simulations, we start with small g and the initial state is $|0\rangle$. After that, we augment g and we use the ground state for the anterior value of g as input state, and so on.

We work with $L = 20$, $L_0 = 10$, $\epsilon = 1$, $J = 1/\pi$, $\Omega = 1$ and $g = 0.05, 0.10, \ldots, 1.00$. The algorithm is considered to converge if the difference between subsequent values of the energy is smaller than 10^{-10} and the difference between subsequent values of the variance $\langle H^2\rangle - \langle H\rangle^2$ is smaller than 10^{-6}. On the other hand, we have again the problem of the infinite Hilbert space on each site, since we are dealing with bosons and there can be any number of excitations, so we have to truncate the local dimension d. We take $d = 8$ in the qubit position and it decays through the line till it achieves $d = 3$. A posteriori, we check that this works, since the number of excitations on each site is much smaller than the local value of d. For the matrix sizes, we choose $D = 6$ in the middle, $D = 1$ in the limits of the chain and $D = 2$ in the rest.

We show the number of excitations in the figure (11). It achieves its maximum at the qubit position and decays exponentially along the chain. Furthermore, as g increases, the maximum becomes higher. Finally, as it is seen, it practically vanishes before arriving to the boundaries, so these ground states are the same for larger values of the length (if we took larger values of g, we would have to take larger chains).

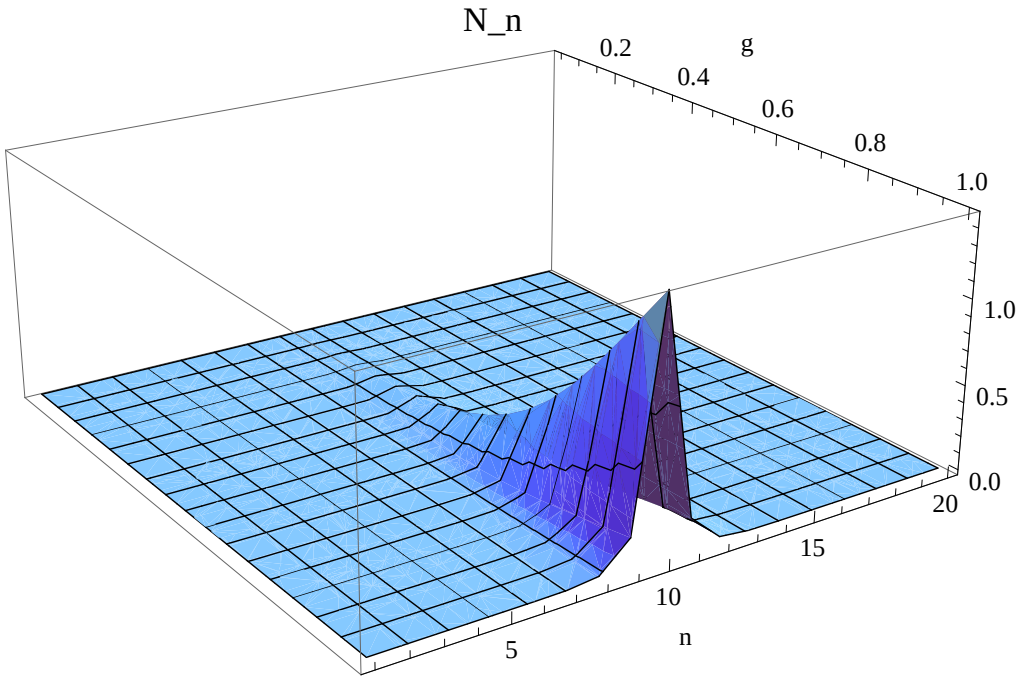

Figure 11: Population of each cavity as a function of the coupling constant g. Clearly, the peak is an increasing function of g.

We show the energy of the ground state vs the coupling constante g in the figure (12). As one can realise, it seems the points lie over a soft curve. If it is true, it implies that there is no crossing between the ground state and the first excited one as g increases. In [28] they prove that this is true for $L = 1$ (the Rabi model). Our result would suggest that it is true even for larger values of L. In addition, again in [28], they obtain a behaviour of the energy as a function of g qualitatively like our result.

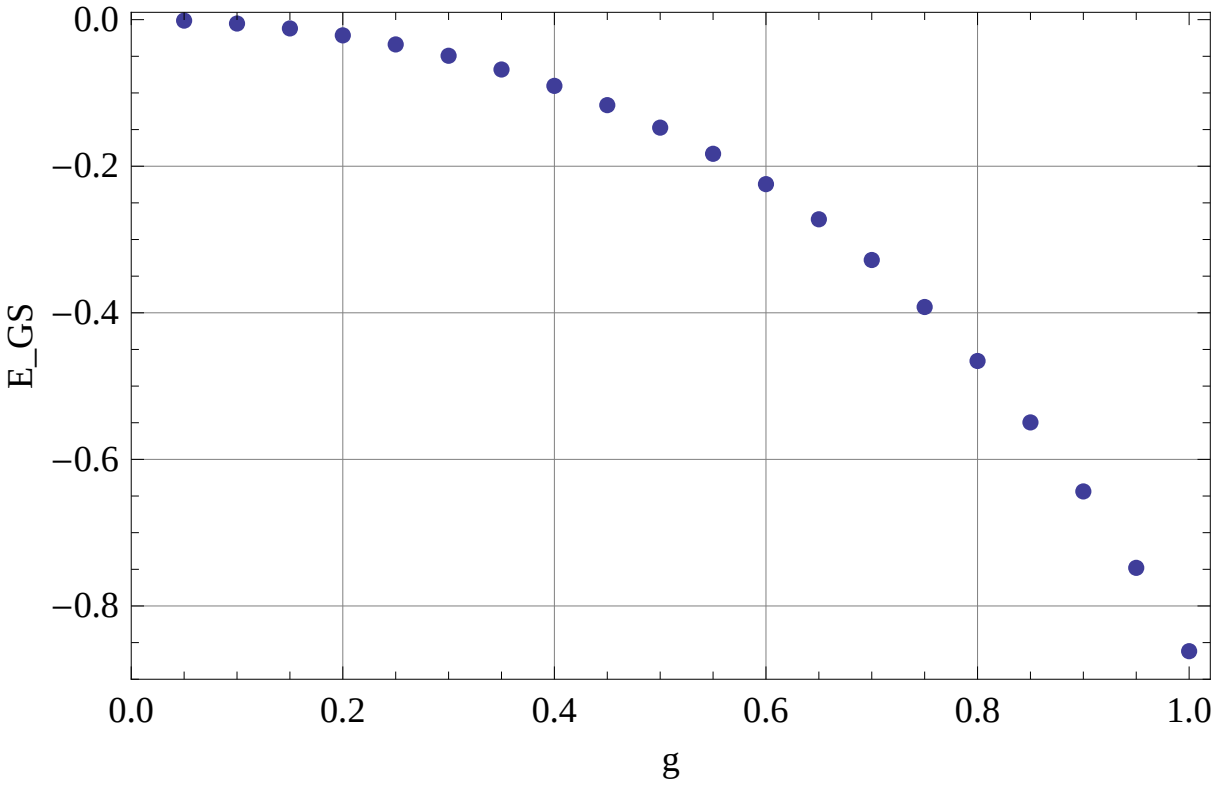

Figure 12: Energy of the ground state as a function of g.

3.4.2 Scattering

Once we have the ground state, we study scattering. Since we took $g = 0.50$ in the RWA case, here we choose the same value for the coupling constant in order to compare the results. For the rest of the parameters, we take again the same values as we took in the RWA case (length of the chain, qubit position, width of the wave packet, etc.).

Now, for the local dimensions of the Hilbert space, we take the same as we took for the search of the ground state and we impose $d = 2$ in the rest of the chain, since we expect that, even though the number of excitations is not conserved, the generated excitations remain close to the qubit. On the other hand, we take $D = 9$ in the middle and it decays until it is $D = 2$ in the rest of the chain, except for the limits, where $D = 1$. Because of the limited computational resources, now we need to take $\Delta t = 0.1$. When truncating we stop it if the error is smaller than 10^{-6} or if a whole sweep has been realised. Then, now the results will not be so clean. This is because the error sources are bigger, since the truncation error is higher, the time step is larger and the initial state is not the desired state since there is a little distance between it and the ground state.

At the moment we do not have a deep comprehension of the system and we need to gather more data, but we have found interesting behaviours for different values of the incident momentum. We show some of the most significant results for the qubit population in the figure (13). First, note that, before interacting, the qubit population is not zero, since the ground state of the system is not $|0\rangle$. In addition, note that the curves

are now slightly noisy because of the error sources which we mentioned above. Now, we analyse the results. First, for the smallest values of k, the qualitative behaviour is that we observed for the RWA case: the qubit population increases and after that it goes again the its ground state ($k = 1.17$ in the figure). However, as it increases, the qubit experiences some kind of slow decay ($k = 1.52$ in the panel). If k is increased, it exhibits again the RWA-like behaviour ($k = 1.32$. However, after that it again has a new kind of behaviour: it decays slowly but, in addition, it seems that it emits and absorbs again and again part of the excitations ($k = 1.72$ in the plot).

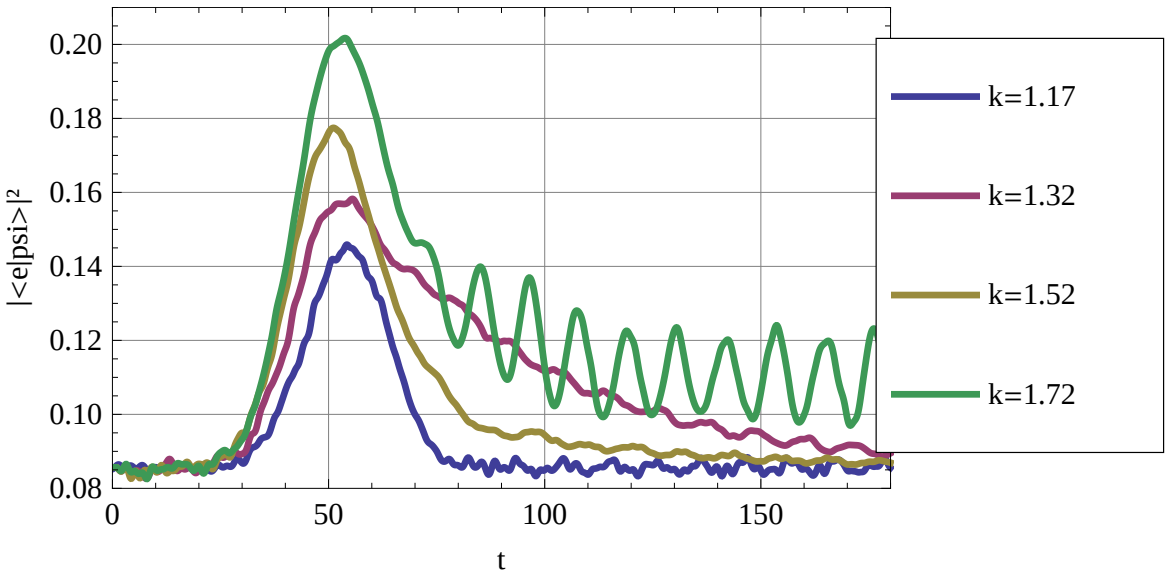

Figure 13: Qubit population vs time in the ultra-strong coupling regime. For different values of the momentum, qualitatively different behaviours appear.

We graph also contour plots with the number of excitations as functions of time and chain position in the figure (14). The left panels ($k = 1.17$ and $k = 1.52$) show the normal behaviour: the wave packet splits in transmitted and reflected parts and the rest of the system comes back to the ground state (note that the excitations in the middle are equal before and after the interaction with the wave packet). However, in the top right graphic ($k = 1.52$) clearly the system does not go immediately to its ground state, but it decays slowly. Finally, in the bottom right panel ($k = 1.72$) the behaviour is even stranger, since the state in the middle exhibits oscillations, as it happens for the qubit, and in addition it emits subsequent pulses.

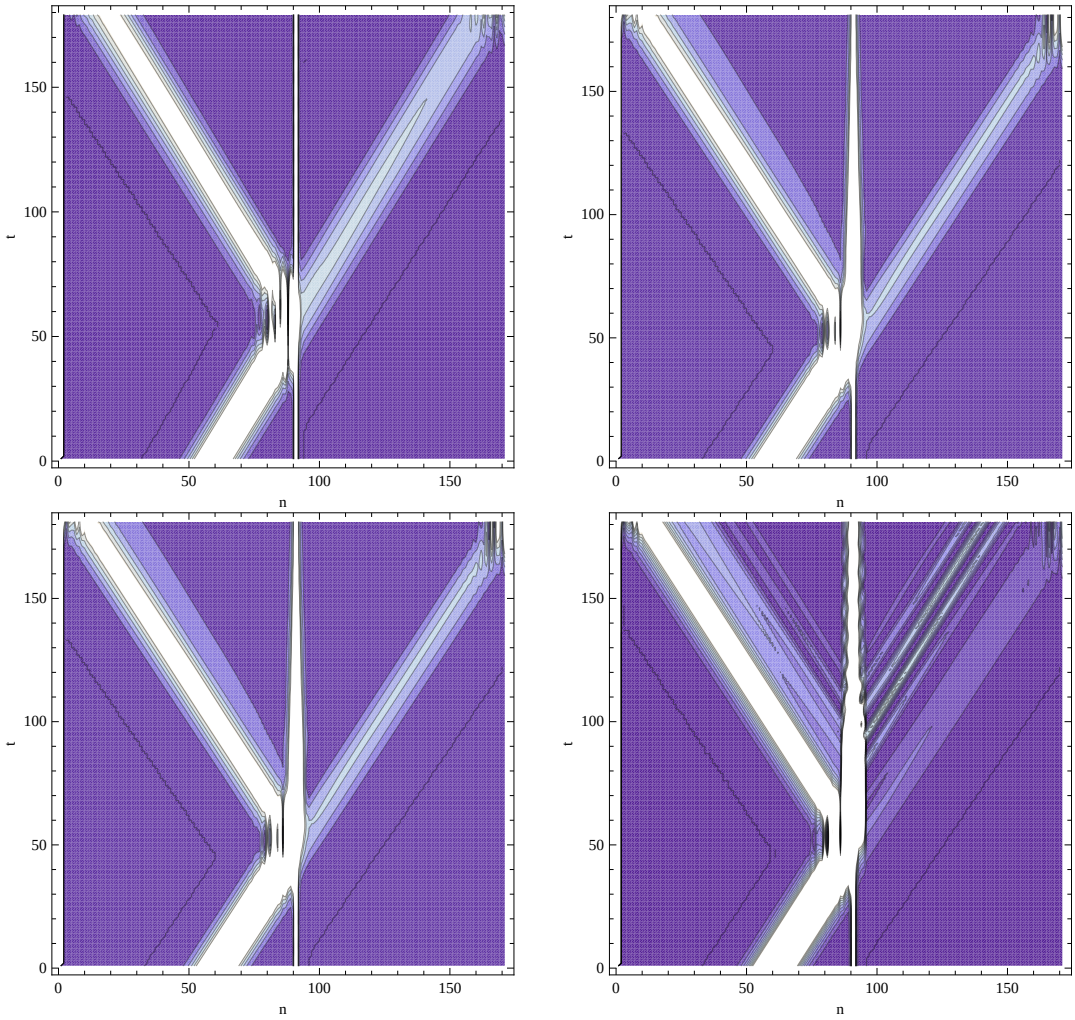

Figure 14: *Contour plots showing the number of excitations as functions of time and position. Top left:* $k = 1.17$*, top right:* $k = 1.32$*, bottom left* $k = 1.52$ *and bottom right* $k = 1.72$*.*

Currently we need to perform a deeper study of the system in order to gain a real comprehension on the behaviour. Anyway, what is clear is that we have found qualitatively different properties respect to those of the RWA regime.

4 Summary, conclusions and future prospects

We have studied the MPS method, one of the most celebrated and powerful numerical techniques in 1D discrete quantum mechanical systems. We have applied it to some simple problems about boson-qubit interactions, obtaining satisfactory results, even beyond RWA.

This work provides some conclusions. First, it is clear that a deep experimental improvement is fundamental to enhance the corresponding theoretical study. Secondly, one more time it becomes evident that totally different branches in physics, as they are black hole physics, quantum information theory or condensed matter physics, can influence

each other.

As future prospects, we shall implement a technical but important tool: absorbing boundary conditions in order to consider larger computation times, since otherwise our system feels the undesired boundary effects. Between the proposals, we are thinking about imposing complex values for the eigenenergies of the Tight Binding Hamiltonian (42) in both ends of the chain, since it would imply a non-Hermitian evolution and, if they were implemented properly, the propagating wave packet would be absorbed. Another option is to follow the proposal of [29], where they introduce a 3 level system interacting with the wave guide via an excited and a metastable level in the RWA approximation, whereas the excited state decays to the ground state because of a non-Hermitian interaction.

On the other hand, we will attack other systems, like scattering in the RWA with more than one photon impinging on different qubits configurations, like one or two qubits, a disorder distribution, etc. For example, right now we are obtaining the first results for 2 photons and 2 separated qubits. In addition, we can consider other kind of problems, like looking for ground states in order to find quantum phase transitions of different 1D strongly correlated systems, or even low-energy excitations spectrum.

Finally, we thank Juan José García Ripoll (Instituto de Física Fundamental, CSIC) for fruitful discussions and useful explanations.

A Details about the truncation

The problem consists of minimising iteratively a function which is a sum of scalar products (20). During this section, we will consider the generic scalar product $\langle\xi|\chi\rangle$, whose MPS tensors are $A(\xi)$ and $A(\zeta)$ respectively. First of all, since the whole function is minimised with respect to the tensors linked to a given site, we are going to write a scalar product between MPS in the following way:

$$\langle\xi|\zeta\rangle = (v_n^\xi)^\dagger E v_n^\zeta, \tag{56}$$

where v_n^ξ and v_n^ζ are the vectorisations of $A(\xi)^n$ and $A(\zeta)^n$ respectively. Using the MPS representation, this scalar product is:

$$\langle\xi|\zeta\rangle = (A(\xi)_1^{i_1})^*_{k_1,k_2}(A(\xi)_2^{i_2})^*_{k_2,k_3}\dots(A(\xi)_L^{i_L})^*_{k_L,k_1}(A(\zeta)_1^{i_1})_{l_1,l_2}(A(\zeta)_2^{i_2})_{l_2,l_3}\dots(A(\zeta)_L^{i_L})_{l_L,l_1} \tag{57}$$

We rewrite it in the following way:

$$\langle\xi|\zeta\rangle = (A_L)_{k_1,l_1,k_n,l_n}(A(\xi)_n^{i_n})^*_{k_n,k_{n+1}}(A(\zeta)_n)^{i_n}_{l_n,l_{n+1}}(A_R)_{k_{n+1},l_{n+1},k_1,l_1}, \tag{58}$$

where A_L and A_R are:

$$(A_L)_{k_1,l_1,k_n,l_n} := (A(\xi)_1^{i_1})^*_{k_1,k_2}(A(\zeta)_1^{i_1})_{l_1,l_2}\dots(A(\xi)_{n-1}^{i_{n-1}})^*_{k_{n-1},k_n}(A(\zeta)_{n-1}^{i_{n-1}})_{l_{n-1},l_n} \tag{59}$$

$$(A_R)_{k_{n+1},l_{n+1},k_1,l_1} := (A(\xi)_{n+1}^{i_{n+1}})^*_{k_{n+1},k_{n+2}}(A(\zeta)_{n+1}^{i_{n+1}})_{l_{n+1},l_{n+2}}\dots(A(\xi)_L^{i_L})^*_{k_L,k_1}(A(\zeta)_L^{i_L})_{l_L,l_1} \tag{60}$$

Now, another tensor C is introduced:

$$C_{k_{n+1},l_{n+1},k_n,l_n} := (A_R)_{k_{n+1},l_{n+1},k_1,l_1}(A_L)_{k_1,l_1,k_n,l_n} \tag{61}$$

Then, the scalar product becomes:

$$\langle\xi|\zeta\rangle = (A(\xi)^{i_n})^*_{k_n,k_{n+1}} C_{k_{n+1},l_{n+1},k_n,l_n} A(\zeta)^{i_n}_{l_n,l_{n+1}} \tag{62}$$

We introduce a Kronecker delta because of convenience:

$$\langle\xi|\zeta\rangle = (A(\xi)^{i_n})^*_{k_n,k_{n+1}} C_{k_{n+1},l_{n+1},k_n,l_n} \delta_{i_n,j_n} A(\zeta)^{j_n}_{l_n,l_{n+1}} \tag{63}$$

Another tensor is defined:

$$D_{k_n,i_n,k_{n+1},l_n,j_n,l_{n+1}} := C_{k_{n+1},l_{n+1},k_n,l_n}\delta_{i_n,j_n} \tag{64}$$

Then:

$$\langle\xi|\zeta\rangle = (A(\xi)^{i_n}_n)^*_{k_n,k_{n+1}} D_{k_n,i_n,k_{n+1},l_n,j_n,l_{n+1}} (A(\zeta)^{j_n}_n)_{l_n,l_{n+1}} \tag{65}$$

Finally, we can define the vectorisations $A(\xi)_n$ by joining all the indices:

$$(v^\xi_n)_{[k_n,i_n,k_{n+1}]} := (A(\xi)^{i_n}_n)^*_{k_n,k_{n+1}}, \tag{66}$$

and the same for v^ζ_n. Here, $[k_n, i_n, k_{n+1}]$ is again a single index, in such a way that we construct a vector from a tensor with three indices (the same for v^ζ_n). In the same way, we define a matrix E by joining the indices of the tensor D in two sets:

$$E_{[k_n,i_n,k_{n+1}],[,l_n,j_n,l_{n+1}]} := D_{k_n,i_n,k_{n+1},l_n,j_n,l_{n+1}} \tag{67}$$

Then, the scalar product is:

$$\langle\xi|\zeta\rangle = (v^\xi_n)^*_{[k_n,i_n,k_{n+1}]} E_{[k_n,i_n,k_{n+1}],[,l_n,j_n,l_{n+1}]} (v^\zeta_n)_{[,l_n,j_n,l_{n+1}]}, \tag{68}$$

or, in vectorial notation:

$$\langle\xi|\zeta\rangle = (v^\xi_n)^\dagger E v^\zeta_n \tag{69}$$

So, we achieve a result like (21), as we wanted to show, as well as the form in which the matrix E has to be constructed.

References

[1] Y.L.A. Rezus, S.G. Walt, R. Lettow, A. Renn, G. Zumofen, S. Gotzinge & and V. Sandoghdar, Physical Review Letters 108, 093601 (2012), *Single-Photon Spectroscopy of a Single Molecule*

[2] O. Astafiev, A.M. Zagoskin, A.A. Abdumalikov Jr., Yu. A. Pashkin, T. Yamamoto, K. Inomata, Y. Nakamura & J. S. Tsai, Science 327, 840-842 (2010), *Resonance Fluorescence of a Single Artificial Atom*

[3] Io-Chun Hoi, C.M. Wilson, G. Johansson, T. Palomaki, B. Peropadre & P. Delsing, Physical Review Letters 107, 073601 (2011), *Demonstration of a Single-Photon Router in the Microwave Regime*

[4] M. D. Eisaman, A. André, F. Massou, M. Fleischhauer, A. S. Zibrov1 & M. D. Lukin, Nature, Vol. 438, Pages 837-841 (2005), *Electromagnetically induced transparency with tunable single-photon pulses*

[5] S. Ritter, C. Nolleke, C. Hahn, A. Reiserer, A. Neuzner, M. Uphoff, M. Mucke, E. Figueroa, J. Bochmann & G. Rempe, Nature 484, 195-201 (2012), *An elementary quantum network of single atoms in optical cavities*

[6] M.S. Tame, K.R. McEnery, S.K. Özdemir, J. Lee, S.A. Maier & M.S. Kim, Nature Physics 2615, 329-340 (2013) *Quantum plasmonics*

[7] C. Eckart, & G. Young, Psychometrika 1 (3): 211–8 (1936), *The approximation of one matrix by another of lower rank*

[8] Claude Cohen-Tannoudji, Bernard Diu & Franck Laloë, *Quantum Mechanics. Volume 1*, Wiley VCH (2006)

[9] Guifré Vidal, Physical Review Letters, Vol 91, Num 14 (2003), *Efficient Classical Simulation of Slightly Entangled Quantum Computations*

[10] Charles H. Bennett, Herbert J. Bernstein, Sandu Popescu & Benjamin Schumacher, Physical Review A, Vol. 53, Nº 40 (1996), *Concentrating partial entanglement by local operations*

[11] F. Verstraete , J.I. Cirac & V. Murga, arXiv: 0907.2996v1 [quant-ph] (2009), *Matrix Product States, Projected Entangled Pair States, and variational renormalization group methods for quantum spin systems*

[12] David Poulin, Angie Qarry, Rolando Somma & Frank Verstraete, Physical Review Letters 106, 170501 (2011), *Quantum Simulation of Time-Dependent Hamiltonians and the Convenient Illusion of Hilbert Space*

[13] J. Eisert, M. Cramer & M. B. Plenio, Reviews of Modern Physics, Vol. 82, Pages 277-306 (2010), *Colloquium: Area laws for the entanglement entropy*

[14] L. Bombelli, R. K. Koul, J. Lee and R. D. Sorkin, Physical Review D Vol. 34, Nº 373. (1986), *Quantum source of entropy for black holes*

[15] Keneth G. Wilson, Reviews of Modern Physics, Vol. 47, Nº 4 (1975), *The renormalization group: Critical phenomena and the Kondo problem*

[16] S. R. White. Physical Review Letters, Vol. 69, Nº 19 (1992), *Density Matrix Formulation for Quantum Renormalization Groups*

[17] J. Ignacio Cirac & Frank Verstraete, J. Phys. A: Math. Theor. 42 (2009) 504004 (34pp), *Renormalization and tensor product states in spin chains lattices*

[18] M. C. Bañuls, K. Cichy, K. Jansen, & J.I. Cirac, arXiv:1305.3765v1 [hep-lat] (2013), *The mass spectrum of the Schwinger model with Matrix Product States*

[19] Juan José García-Ripoll, New Journal of Physics 8 (2006) 305, *Time evolution of Matrix Product States*

[20] Ian P. McCulloch, Journal of Statistical Mechanics: Theory and Experiment, P10014 (2007), *From density-matrix renormalization group to matrix product states*

[21] Claude Cohen-Tannoudji, Jacques Dupont-Roc & Gilbert Grynberg, *Photons and Atoms: Introduction to Quantum Electrodynamics*, Wiley Professional (2004)

[22] Kazuyuki Fujii, arXiv:1301.3582v2 [quant-ph] (2013), *Introduction to the Rotating Wave approximation (RWA): Two Coherent Oscillations*

[23] Juan José García-Ripoll & David Zueco, *Transmission line discretisation* (not published notes)

[24] Alexander Altland & Ben Simons, *Condensed Matter Field Theory*, Cambridge University Press, 2nd edition (2010)

[25] Lan Zhou, H. Dong, Yu-xi Liu, C.P. Sun, and Franco Nori, Physical Review A 78, 063827 (2008), *Quantum supercavity with atomic mirrors*

[26] T. Niemczyk, F. Deppe, H. Huebl, E.P. Menzel, F. Hocke, M.J. Schwarz, J.J. García-Ripoll, D. Zueco, T. Hümmer, E. Solano, A. Marx & R. Gross, Nature Physics 6, 772–776 (2010)*Circuit quantum electrodynamics in the ultrastrong-coupling regime*

[27] B. Peropadre, P. Forn-Díaz, E. Solano & J.J. García-Ripoll, Physical Review Letters 105, 023601 (2010), *Switchable Ultrastrong Coupling in Circuit QED*

[28] Masao Hirokawa & Fumio Hiroshima, arXiv:1207.4020v1 [math-ph] (2012), *Absence of Energy Level Crossing for the Ground State Energy of the Rabi Model*

[29] B. Peropadre, G. Romero, G. Johansson, C. M. Wilson, E. Solano & J.J. García-Ripoll, Physical Review A, Vol 84, Num 063834 (2011), *Approaching perfect microwave photodetection in circuit QED*

[30] María Gracia Eckholt Perotti, thesis realised at Technische Universität München and at Max-Planck-Institut für Quantenoptik, directed by J.I. Cirac, M. Wolf & J.J. García Ripoll (2005), *Matrix Product Formalism*

[31] Guifré Vidal, Physical Review Letters, Vol 93, Num 4 (2004), *Efficient Simulation of One-Dimensional Quantum Many-Body Systems*